Desalination and Water Treatment
www.deswater.com

doi: 10.1080/19443994.2014.903873

54 (2015) 1281–1289
April

Taylor & Francis
Taylor & Francis Group

Effects of groundwater solutes on colloidal stability of polymer-coated and bare nanosized zero-valent iron particles

Cheolyong Kim[a], Jun-Young Ahn[a], Kyung-Yup Hwang[a], Hong-Seok Kim[b], Dae-Young Kwon[c], Inseong Hwang[a,*]

[a]*School of Civil and Environmental Engineering, Pusan National University, 30 Jangjeon-dong, Geumjeong-gu, Busan, Republic of Korea, Tel. +82 51 510 3523; Fax: +82 51 514 9574; email: ihwang@pusan.ac.kr*
[b]*Water & Environment R&D Team, Research & Development Division, Hyundai Engineernig & Construction Co., Ltd, 17-6, Mabuk-ro 240-gil, Giheung-gu, Yongin-si, Gyeonggi-do, Republic of Korea*
[c]*Department of Civil and Urban Engineering, Inje University, 607 Eobang-dong, Gimhae, Gyeongnam, Republic of Korea*

Received 15 January 2014; Accepted 5 March 2014

ABSTRACT

Colloidal stabilities of polymer-coated nanosized zero-valent iron (pNZVI) and bare nanosized zero-valent iron (bNZVI) particles were investigated in the presence of groundwater solutes, such as Suwannee River natural organic matter (SRNOM), Pony Lake fulvic acid (PLFA), sodium ion, and calcium ion. Measurements of hydrodynamic diameter and zeta-potential showed that dissolved organic matters (SRNOM and PLFA) enhanced the stability of bNZVI particles, but that they did not affect the stability of pNZVI particles. These measurements also showed that the stability of pNZVI particles was inhibited by the cations but that the effect of the cations on bNZVI particles was inconclusive. The sedimentation test confirmed that the stability of pNZVI particles was inhibited by the sodium and calcium ions. The sedimentation test identified that the stability of bNZVI particles was inhibited only in the presence of calcium ion. The predictions on the stability of NZVI particles based on the Derjaguin–Landau–Verwey–Overbeek interaction energies were generally consistent with experimental observations. Energy barriers of bNZVI particles were estimated to be up to 7.5 and 91 k_BT in the presence of PLFA and SRNOM, respectively. For pNZVI particles, energy barriers were present in all experimental conditions except for the suspension with calcium ion.

Keywords: Nanosized zero-valent iron; Colloidal stability; Dissolved organic matter; Cations; Aggregation

1. Introduction

For over a decade, nanosized zero-valent iron (NZVI) particles have received attention due to their outstanding effectiveness in treating environmental contaminants. Large specific surface area of NZVI resulting from its small size provides a broad site for chemical reaction and adsorption [1,2]. Therefore, NZVI can effectively treat various groundwater

---

*Corresponding author.

Presented at the 6th International Conference on the "Challenges in Environmental Science and Engineering" (CESE-2013), 29 October–2 November 2013, Daegu, Korea

contaminants, e.g. chlorinated solvents and heavy metals, through suitable mechanisms, e.g. reduction, precipitation, oxidation, and adsorption [3–6]. Its small size, moreover, provides advantages with respect to mobility in the subsurface during groundwater remediation. Well-dispersed iron nanoparticles can migrate through pores of the aquifer and target onto contaminants more effectively than conventional microsized zero-valent iron particles. It is very important to maintain the colloidal stability of NZVI when it is injected into the subsurface for contaminated source control [7].

Bare NZVI (bNZVI) is generally unstable in water due to van der Waals and magnetic attractive forces among particles, which are higher than electrostatic repulsion [7,8]. Since bNZVI has poor stability in water dispersion, several techniques for improving colloidal stability have been developed [9–12]. Nonionic surfactants and natural and synthetic polymers have been considered as stabilizing agents in many studies. These kinds of organic materials were used as surface coatings of NZVI to enhance electrostatic and steric repulsion of dispersed particles. Consequently, the organically coated NZVI showed improved stability in dispersion. Among the stabilizers, the synthetic polymers are especially effective and readily available for practical applications.

Although the stability of NZVI can be enhanced by surface coatings, such as polymers, it still remains doubtful that NZVI can maintain its stability during its application in the natural environment. This is because the stability of NZVI is affected not only by the intrinsic characteristics of particles but also by the conditions of circumferential dispersants. Several studies have been conducted to predict the NZVI stability in natural environments using various methods including sedimentation test and calculation of Derjaguin–Landau–Verwey–Overbeek (DLVO) interaction energy between particles [10,11,13,14]. Saleh et al. revealed that sodium and calcium ions inhibited stability. Johnson et al. and Chen et al. reported that dissolved organic matter (DOM) enhanced stability of NZVI [15,16]. Albeit previous studies reported on the effect of some groundwater components on NZVI, the scopes of studies were confined to laboratory-synthesized NZVI and a minority of commercial NZVI. Nanofer is a commercial NZVI and is becoming a very popular field-applied agent worldwide. Therefore, there is an urgent need to investigate its stability in the natural environment for its successful field application.

This study aims to investigate the effect of groundwater solutes including cations and DOMs on the stability of bare and polymer-coated Nanofer products. Colloidal properties of particles, such as hydrodynamic diameter and zeta-potential, were measured to predict static characteristics of NZVI suspensions. Sedimentation tests were then conducted to investigate kinetic colloidal behaviors of NZVI. Finally, DLVO interaction energies between particles under different dispersant conditions were calculated to estimate interparticle forces that are composed of electrical double-layer repulsion and van der Waals attraction [17].

2. Materials and methods

2.1. Preparation of NZVI samples

Nanofer 25 and Nanofer 25S (Nanoiron, Czech Republic), which are commercially available NZVIs were used as a bNZVI and a polymer-coated NZVI (pNZVI), respectively. Nanofer 25 is in a strict sense not the bNZVI because it is modified with traces of unidentified inorganic material. However, the contribution of the inorganic matter to changes in the stability of NZVI is supposed to be negligible. Therefore, Nanofer 25 is referred to as bNZVI. The surface of Nanofer 25S was coated with Na-polyacrylic acid (PAA) according to the information from the manufacturer. Lerner et al. identified that Nanofer 25S was fully covered with Na-PAA because strong peaks representing carbon, oxygen, and sodium bonding were observed by auger electron spectroscopy and X-ray photoelectron spectroscopy [14].

Solutions of cations or DOMs were prepared to simulate natural groundwater conditions. Cationic solutions contained 2 mN of sodium or calcium ion as chloride salts (99.5%, Junsei, Japan). Two types of standard DOMs, Suwannee River natural organic matter (SRNOM) and Pony Lake fulvic acid (PLFA), were purchased from International Humic Substances Society and prepared as 20 mg/L solutions. Before relevant NZVI dispersions were prepared, the pH of each solution was adjusted to 8.0 to minimize pH changes during the tests. The dispersants including DI water were deoxygenized to exclude the effect of oxygen. Controls represent NZVI dispersions in DI water without groundwater solutes. Each type of NZVI was injected into dispersants to yield a concentration of 1 g/L. Samples were transferred to 24 mL borosilicate vials with a Teflon-lined cap, and the volume of each sample was 20 mL. The vials were mounted on a rotary shaker and rotated at 20 rpm for 5 d to give enough interaction between particle and dispersant.

2.2. Sedimentation test

After NZVI was equilibrated with each dispersant for 5 d, samples were taken and diluted to 100 mg

NZVI/L into corresponding dispersants. Kinetics of NZVI sedimentation were investigated using a time-resolved spectroscopy (Optizen 3220UV, Mecasys). UV absorbances of the NZVI samples at 508 nm were measured at a 15 s interval for 30 min [7]. The measured absorbances were normalized with initial absorbances of control samples.

2.3. Measurement of hydrodynamic diameter and zeta-potential

The hydrodynamic diameter and zeta-potential were measured using a Zetasizer (Nano ZS, Malvern). The samples were prepared same as was done in the sedimentation test. Hydrodynamic diameter of particles was measured by dynamic light scattering at 633 nm. Zeta-potential of particles was estimated from the electrophoretic mobility of particles.

2.4. Calculation of DLVO interaction energy

DLVO interaction energies of particles were calculated. DLVO energy is the sum of energies resulting from electrical double-layer repulsion and van der Waals attraction. Electrical double-layer repulsion energy (V_{EDL}) was estimated using Eq. (1) [18].

$$V_{\mathrm{EDL}} = 2\pi\varepsilon_{\mathrm{r}}\varepsilon_0 a\zeta^2 \ln[1 + \mathrm{e}^{-\kappa}h] \tag{1}$$

κ^{-1} is the Debye length of particles and defined as the following Eq. (2) [19]:

$$\kappa^{-1} = \sqrt{\frac{\varepsilon_{\mathrm{r}}\varepsilon_0 k_{\mathrm{B}}T}{2N_{\mathrm{A}}\mathrm{e}^2 I}} \tag{2}$$

van der Waals attraction energy between particles was calculated using Eq. (3) [20].

$$V_{\mathrm{vdW}} = \frac{-A}{6}\left[\frac{2a^2}{h(4a+h)} + \frac{2a^2}{(2a+h)^2} + \ln h\frac{(4a+h)}{(2a+h)^2}\right] \tag{3}$$

The meanings of the variables in the equations and the values used are presented in Table 1. The total DLVO energy was plotted against separation distance (h) of particles and the stability of NZVI was evaluated according to the energy profile.

3. Results and discussions

3.1. Colloidal properties

Hydrodynamic diameter and zeta-potential of colloidal particles are directly related to stability of the particles. Results of the measurements for the two parameters are shown in Fig. 1. In general, hydrodynamic diameters of bNZVI were larger than those of pNZVI under all dispersant conditions. The higher hydrodynamic diameter resulted from more aggregation of bNZVI particles. This verified that pNZVI had better stability than bNZVI. Hydrodynamic diameter of bNZVI evidently decreased in the presence of DOMs. It was supposed that DOMs covered the surface of particles and enhanced electrostatic and steric repulsions. It is also shown that bNZVI was more stable in the SRNOM solution than in the PLFA solution. This is believed to be resulted from differences in characteristics of two DOMs. SRNOM has a larger molecular weight than PLFA and is more hydrophobic than PLFA [21]. Therefore, SRNOM with more functional groups should have provided greater steric hindrance than PLFA. In addition, relatively higher hydrophobicity of SRNOM appeared to make particles dispersed better than PLFA [17,22–24]. On the other hand, cations do not appear to affect hydrodynamic diameter of bNZVI. It is speculated that aggregated particles were thermodynamically stable in the size ranges around 3,000 nm of hydrodynamic diameter.

While bNZVI was stabilized by DOMs, the effects of DOMs on the hydrodynamic diameter of pNZVI were not evident. Fig. 1 shows the hydrodynamic diameter of pNZVI slightly increased in the SRNOM solution. In contrast to the result of bNZVI experiments, stability of pNZVI did not increase in the presence of DOMs. It is reasonable to assume that the surface of particles had been already saturated with the polymer coating, hence no more sorption site was available for DOMs. With regard to the effects of cations, hydrodynamic diameter of pNZVI was not affected by sodium ion but by calcium ion. Hydrodynamic diameter of particles under the effect of calcium was 8.7-fold larger than that in DI water. Divalent cations, such as calcium can further reduce the double-layer repulsion of colloid particles than monovalent cations, thus particle stability was more inhibited by calcium ion than sodium ion.

Results of the zeta-potential measurement were comprehensively consistent with those of hydrodynamic diameter. As shown in Fig. 1(b), pNZVI generally exhibited higher magnitudes of zeta-potential than bNZVI. Magnitudes of zeta-potential of bNZVI particles increased in the presence of DOMs. On the

Table 1
Parameters and their values for DLVO calculation

	Interpretation (unit)	Value
ε_0	Vacuum permitivity (F/m)	8.85E − 12
ε_r	Relative permitivity of water (–)	78.54
a	Hydrodynamic diameter of NZVI (m)	Measured
ζ	Zeta-potential of NZVI (mV)	Measured
e	Electron charge (C)	1.602E − 19
N_A	Avogadro's number (/mol)	6.02E + 23
k_B	Boltzmann constant (J/K)	1.38E − 23
T	Absolute temperature (K)	293
A	Hamaker constant (J)	8.0E − 20
I	Ionic strength (mol/m^3)	For each solution

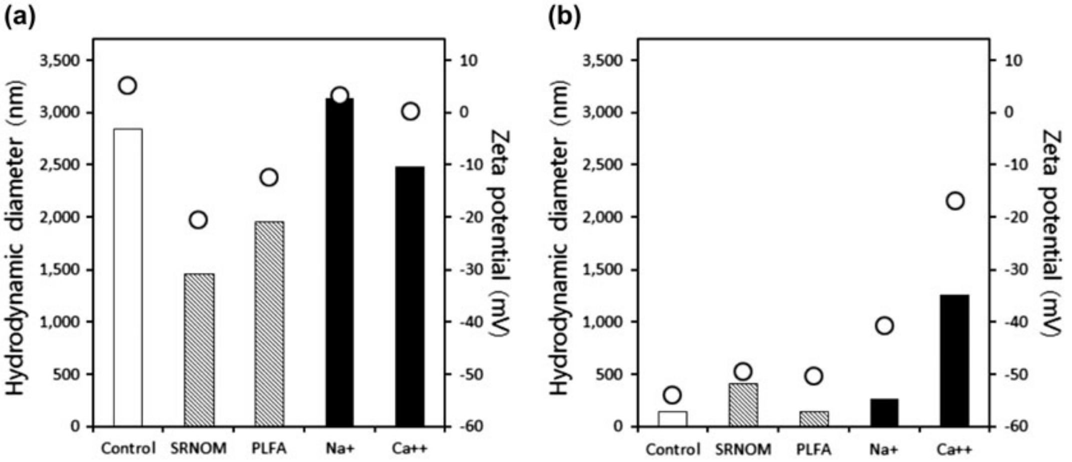

Fig. 1. Hydrodynamic diameters (bar) and zeta-potentials (bullet) of (a) bNZVI particles, and (b) pNZVI particles in various dispersants.

other hand, zeta-potential of bNZVI in the solution of calcium ion completely disappeared, which confirmed the well-known effect of cation on the double-layer repulsion. Consistent with the results of hydrodynamic diameter, DOMs did not affect the zeta-potential values of pNZVI substantially. However, calcium ion drastically decreased the magnitude of zeta-potential. Sodium ion also substantially decreased the magnitude of zeta-potential of pNZVI, which means that monovalent ion as well as divalent ion can affect electrostatic repulsion of pNZVI particles.

3.2. Sedimentation characteristics

Normalized sedimentation curves of bNZVI and pNZVI suspensions are presented in Fig. 2. It is notable that initial absorbances of the suspensions were different for different dispersant conditions. Compared to the control sample, for example, the initial absorbance of bNZVI in the SRNOM solution was higher. This suggests that the particles were well dispersed in the presence of SRNOM. It can be hypothesized that there were two different fractions of particles. The first fraction was believed to contribute to the initial absorbances. The second fraction was instantaneously excluded from the dispersions before optical measurements were conducted due to their excessively large particle sizes. Relative initial absorbance was defined as the difference between normalized initial absorbance of each sample and that of the relevant control sample. This is an important parameter when assessing the stability of particle and is shown in Fig. 3.

Fig. 3 shows that relative initial absorbances became higher when bNZVI particles were dispersed

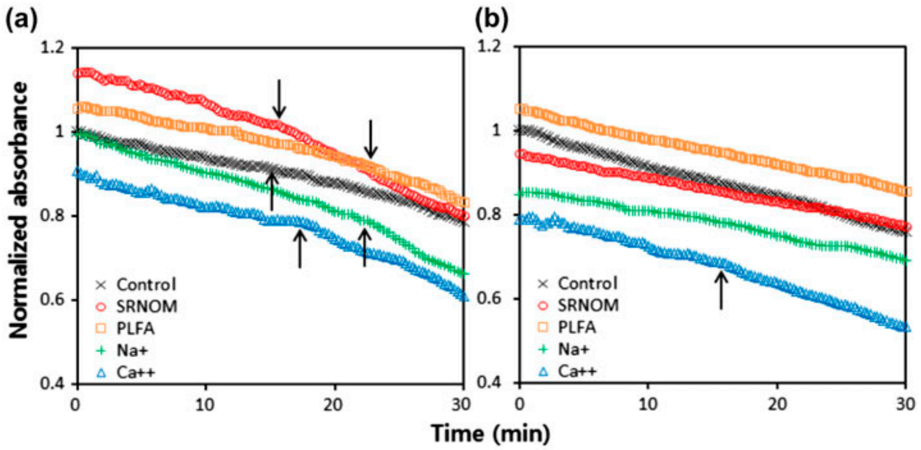

Fig. 2. Sedimentation curves of (a) bNZVI particles, and (b) pNZVI particles in various dispersants. The points marked by arrows are critical times.

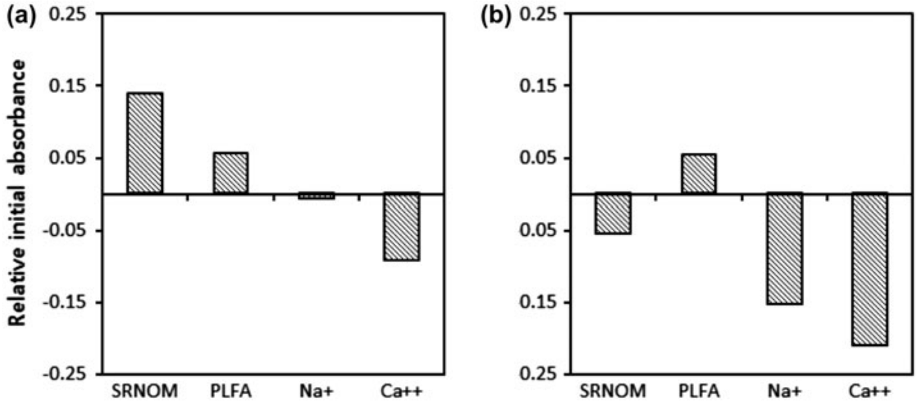

Fig. 3. Relative initial absorbances of (a) bNZVI particles, and (b) pNZVI particles in various dispersants.

in the DOM solutions. This indicates that particles in the DOM solutions were more stable than those in the control sample. It is also seen that SRNOM further enhanced the stability of bNZVI particles than PLFA. Sodium ion did not affect the stability of bNZVI particles. However, calcium ion lowered the relative initial absorbance, which means it lowered the stability. These observations are generally consistent with the changes in colloidal properties of bNZVI particles that were discussed in the subsection 3.1.

In the case of pNZVI experiments, the presence of DOMs produced disputed results. Relative initial absorbance of the pNZVI particles decreased in the presence of SRNOM; in contrast, PLFA enhanced the initial dispersivity of the particles. These observations are in agreement with the changes in hydrodynamic diameter of pNZVI particles in the presence of DOMs (Fig. 1(b)). The particle sizes were increased in the SRNOM solution. It is supposed that SRNOM in this case acted as a coagulant that caused interparticle bridging between pNZVI particles. As was observed in the experiments on the colloidal properties, cations inhibited the initial stability of pNZVI. Compared to the control, the dispersions of pNZVI initially lost 15 and 21% of the particles in the presence of sodium and calcium ions, respectively. This verified that cations, especially calcium ion inhibited double-layer repulsion of pNZVI particles.

Sedimentation kinetics of NZVI particles are also important when evaluating the stability of NZVI particles in addition to the initial absorbance values. In Fig. 2, sedimentation curves of bNZVI particles were divided into two parts based on the changes in the slope. In other words, sedimentation of bNZVI particles fell into two distinct phases. Phenrat et al. reported that two or three regions were observed in the sedimentation curves of NZVI particles according to the slopes of curves. In that study, the first region with gradual slope was considered an aggregation stage and the following region with steep slope a sedimentation stage. Settling rate during the aggregation stage is supposed to be lower due to relatively smaller particle sizes than that during the aggregation stage. The point when aggregation phase changes into sedimentation phase is called critical time [7]. The curves obtained in this study also show similar trends.

To quantify sedimentation rates of NZVI particles, sedimentation curves were fitted using Eq. (4), and characteristic time (τ) was obtained [25].

$$C = C_0 e^{-\frac{t}{\tau}} \tag{4}$$

Concentrations of NZVI particles were assumed to be proportional to the absorbances of dispersions. Fig. 4 shows characteristic times for sedimentation of the NZVI particles. Characteristic time is an inverse of sedimentation rate constant and it is considered as the time required for sedimentation processes to become stable. This means that when the characteristic time is higher, the particles settle slower. In this study, characteristic times of aggregation phase and sedimentation phase were referred as τ_{agg} and τ_{sed}, respectively.

Fig. 4(a) shows that in the case of bNZVI particles, the values for τ_{agg} were 1.4 to 2.5 times higher than those for τ_{sed}. This suggests that bNZVI particles in all conditions were unstable in dispersion and became aggregated further. It is also seen that differences between τ_{agg} and τ_{sed} of bNZVI particles dispersed in the DOM solutions were higher than that of the control. This implies that aggregations of bNZVI particles with DOMs were significant and that the bNZVI particles in the sedimentation test were not as stable as was predicted by the colloidal properties, such as the hydrodynamic diameter and zeta-potential. The discrepancy between the results from two approaches may be due to a number of factors. For example, polymer bridging could be a major factor affecting the stability of NZVI particles in the presence of DOMs [26]. However, this kind of bridging cannot be confirmed by measuring the zeta-potential or hydrodynamic diameter. When bNZVI particles were dispersed in the cationic solutions, differences between τ_{agg} and τ_{sed} of bNZVI particles were generally greater than that of the control. While the results of the measured colloidal properties identified no clear effect of cations on the stability of bNZVI particles, the sedimentation curves showed that bNZVI particles aggregated more actively in the presence of the cations. This indicates that the stability of bNZVI particles was consistently varied by the cations during the sedimentation test. Extensive time-resolved measurements of the colloidal properties of bNZVI particles should be conducted to better characterize a time-dependent effect of the cations. Nonetheless, these results reveal that the cations could make even bNZVI particles more unstable.

In contrast with bNZVI particles, two distinguishable phases of sedimentation were not observed in most of the pNZVI experiments (Fig. 4(b)). Only the experiment under the calcium ion showed τ_{agg} and $\tau_{\mathrm{sed.}}$ Since the other four curves did not have aggregation phases, the characteristic times for sedimentation (τ_{sed}) were only indicated in Fig. 4(b). The absence of two distinct sedimentation phases is believed to be due to the presence of the polymer coating of pNZVI particles that prevented aggregation during the sedimentation tests. Therefore, it is predicted that pNZVI particles can maintain their stability in the presence of DOMs and monovalent cations.

The effect of sodium ion on the sedimentation behavior of pNZVI particles was not obvious in this

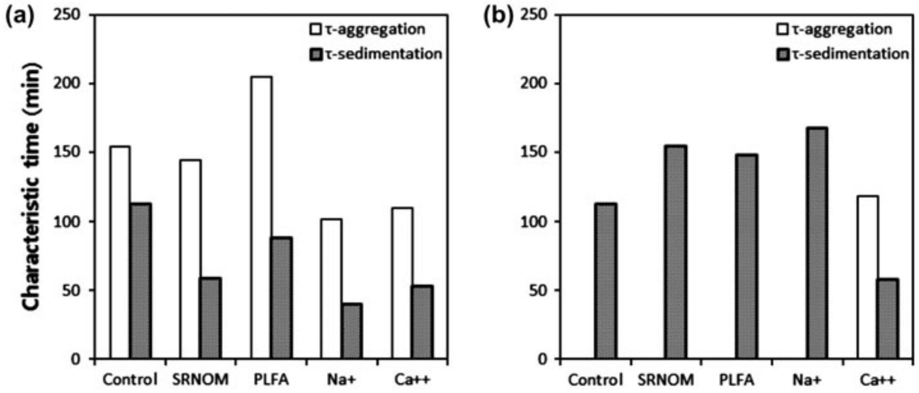

Fig. 4. Aggregation and sedimentation characteristic times for (a) bNZVI particles, and (b) pNZVI particles.

study. However, Tiraferri et al. reported that the sedimentation curve of NZVI particles in 100 mM of sodium ion solution was composed of aggregation and sedimentation phases that were observed in systems containing unstable particles [11]. Based on the current and previous results, it can be asserted that the stability of pNZVI particles is probably not affected by sodium ion with natural surface water concentrations but is affected under excessively high sodium ion concentrations. While pNZVI particles were stable in the sodium solution, two different sedimentation phases were observed in the presence of calcium ion. This is consistent with the results of the measurements of the hydrodynamic diameter and zeta-potential of pNZVI particles under the calcium ion condition. Previous studies also reported that calcium ion with a naturally occurring concentration caused aggregation of NZVI particles [10,11].

3.3. DLVO interaction energy

DLVO interaction energies for NZVI particles provide insights into the stability and aggregation behaviors of NZVI particles in various dispersant conditions. Calculated DLVO energy profiles of bNZVI and pNZVI particles are presented in Fig. 5. DLVO energy of bNVZI in DI water (control) remained negative within the range of 0–100 nm of separation distance. This indicates that bNZVI particles would be unstable in DI water, because negative DLVO energy reflects an attractive force between particles. DLVO energy profiles of bNZVI in the cationic solutions were similar to that of control, suggesting that cations would not significantly affect the stability of bNZVI particles. In the presence of PLFA, the stability of bNZVI particles was slightly enhanced and the interaction energy between particles was almost neutral within the range of 20–100 nm of separation distance. Additionally, there was an energy barrier of up to 7.5 k_BT at the separation distance between 20 and 60 nm. SRNOM is expected to facilitate dispersion of bNZVI particles more effectively than PLFA, because an energy barrier of up to 91 k_BT was observed.

DLVO energy profiles for pNZVI systems show that pNZVI particles would be stable in most dispersant conditions except for the calcium ion solution. PLFA barely affected the DLVO energy profile of pNZVI compared with that in the DI water condition. However, SRNOM drastically extended the energy barrier. Magnitudes of estimated energy barriers were 1.1×10^2, 1.2×10^2, and $2.8 \times 10^2\, k_BT$, in the DI water, PLFA, and SRNOM solutions, respectively. Extension of the energy barrier in the presence of SRNOM was supposed to be due to a thermodynamically stable hydrodynamic diameter of pNZVI particles in the SRNOM solution.

Compared to control, the magnitude of the energy barrier of pNZVI particles was lower in the sodium solution, which was 60 k_BT at a separation distance between 1.4 and 28 nm. pNZVI particles are expected to lose their stability under the effect of calcium ion, although pNZVI particles still maintained the energy barrier in the presence of sodium ion. This prediction is reflected in the results of the sedimentation test for the pNZVI/calcium suspension where an aggregation phase was observed solely among pNZVI experiments. DLVO energy profile proved to be valuable in predicting the stability of NZVI particles in the presence of groundwater solutes, because the model predictions were consistent with the apparent sedimentation behaviors of NZVI particles.

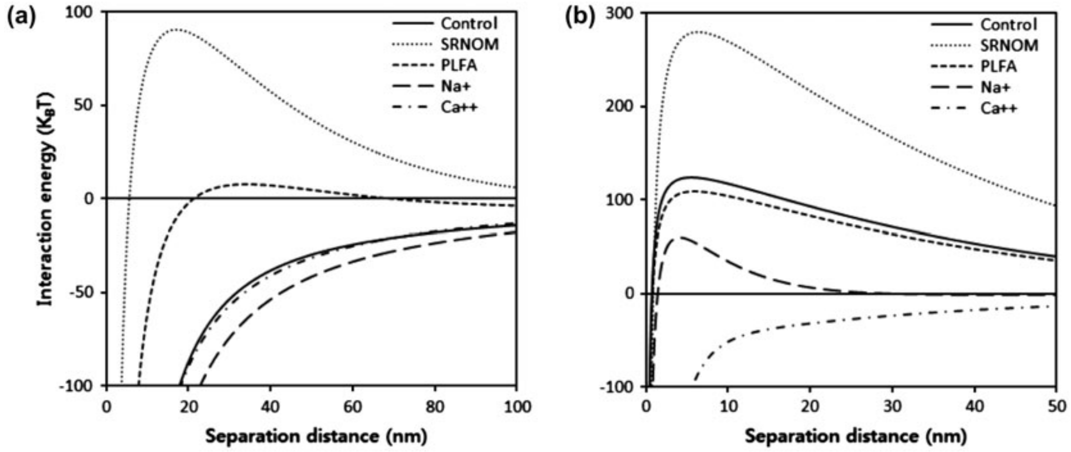

Fig. 5. DLVO energy profiles of (a) bNZVI particles, and (b) pNZVI particles in various dispersants.

4. Conclusions

Colloidal stabilities of pNZVI and bNZVI particles were investigated in the presence of various groundwater solutes. Results of the measurements of hydrodynamic diameter and zeta-potential, and sedimentation tests revealed that pNZVI particles generally had better stability than bNZVI particles in the presence of groundwater solutes. The results of hydrodynamic diameter and zeta-potential measurements showed that the DOMs (SRNOM and PLFA) enhanced the stability of bNZVI particles, but that the effects of DOMs on the stability of pNZVI particles were not obvious. Results of the sedimentation tests were in good agreement with the hydrodynamic diameter and zeta-potential measurements.

The effects of cations on the stability of bNZVI particles were not evident in the results of measurements of hydrodynamic diameter and zeta-potential. The results of the sedimentation test indicated that only calcium ion inhibited the stability of bNZVI particles. The stability of pNZVI particles was decreased by sodium and calcium ions, and the hydrodynamic diameter of the particles with calcium ion was 8.7 times greater than that of control. The sedimentation test confirmed that sodium and calcium ions inhibited the stability of pNZVI particles.

The predictions on the stability of NZVI particles based on the DLVO interaction energies were generally consistent with the experimental observations. The energy barriers of bNZVI particles in the presence of SRNOM and PLFA reach 91 and $7.5\,k_BT$, respectively, predicting the enhancement of the stability of NZVI suspensions. Energy barriers were not observed for bNZVI particles in the other solutes. In the case of pNZVI particles, the energy barriers of up to $60\,k_BT$ were present in most experimental conditions except for the suspension with calcium ion. The energy barriers of the pNZVI particles in DI water or in the presence of SRNOM and PLFA were in an order of magnitude greater than that in the sodium ion solution.

Acknowledgment

This work was supported by national research foundation of korea [grant number KRF-2010-0012992].

References

[1] C. Wang, W. Zhang, Synthesizing nanoscale iron particles for rapid and complete dechlorination of TCE and PCBs, Environ. Sci. Technol. 31 (1997) 2154–2156.

[2] J.T. Nurmi, P.G. Tratnyek, V. Sarathy, D.R. Baer, J.E. Amonette, K. Pecher, C. Wang, J.C. Linehan, D.W. Matson, R.L. Penn, Characterization and properties of metallic iron nanoparticles: Spectroscopy, electrochemistry, and kinetics, Environ. Sci. Technol. 39 (2005) 1221–1230.

[3] Y. Liu, S.A. Majetich, R.D. Tilton, D.S. Sholl, G.V. Lowry, TCE dechlorination rates, pathways, and efficiency of nanoscale iron particles with different properties, Environ. Sci. Technol. 39 (2005) 1338–1345.

[4] X. Li, W. Zhang, Sequestration of metal cations with zerovalent iron nanoparticles – A study with high resolution X-ray photoelectron spectroscopy (HR-XPS), J. Phys. Chem. C 111 (2007) 6939–6946.

[5] Y. Xu, D. Zhao, Reductive immobilization of chromate in water and soil using stabilized iron nanoparticles, Water Res. 41 (2007) 2101–2108.

[6] S. Kang, W. Choi, Oxidative degradation of organic compounds using zero-valent iron in the presence of natural organic matter serving as an electron shuttle, Environ. Sci. Technol. 43 (2008) 878–883.

[7] T. Phenrat, N. Saleh, K. Sirk, R.D. Tilton, G.V. Lowry, Aggregation and sedimentation of aqueous nanoscale zerovalent iron dispersions, Environ. Sci. Technol. 41 (2007) 284–290.

[8] F. He, D. Zhao, Preparation and characterization of a new class of starch-stabilized bimetallic nanoparticles for degradation of chlorinated hydrocarbons in water, Environ. Sci. Technol. 39 (2005) 3314–3320.

[9] B.W. Hydutsky, E.J. Mack, B.B. Beckerman, J.M. Skluzacek, T.E. Mallouk, Optimization of nano- and microiron transport through sand columns using polyelectrolyte mixtures, Environ. Sci. Technol. 41 (2007) 6418–6424.

[10] N. Saleh, H. Kim, T. Phenrat, K. Matyjaszewski, R.D. Tilton, G.V. Lowry, Ionic strength and composition affect the mobility of surface-modified Fe0 nanoparticles in water-saturated sand columns, Environ. Sci. Technol. 42 (2008) 3349–3355.

[11] A. Tiraferri, K.L. Chen, R. Sethi, M. Elimelech, Reduced aggregation and sedimentation of zero-valent iron nanoparticles in the presence of guar gum, J. Colloid Interface Sci. 324 (2008) 71–79.

[12] F. He, D. Zhao, C. Paul, Field assessment of carboxymethyl cellulose stabilized iron nanoparticles for *in situ* destruction of chlorinated solvents in source zones, Water Res. 44 (2010) 2360–2370.

[13] N. Sakulchaicharoen, D.M. O'Carroll, J.E. Herrera, Enhanced stability and dechlorination activity of pre-synthesis stabilized nanoscale FePd particles, J. Contam. Hydrol. 118 (2010) 117–127.

[14] R.N. Lerner, Q. Lu, H. Zeng, Y. Liu, The effects of biofilm on the transport of stabilized zerovalent iron nanoparticles in saturated porous media, Water Res. 46 (2012) 975–985.

[15] R.L. Johnson, G.O. Johnson, J.T. Nurmi, P.G. Tratnyek, Natural organic matter enhanced mobility of nano zerovalent iron, Environ. Sci. Technol. 43 (2009) 5455–5460.

[16] J. Chen, Z. Xiu, G.V. Lowry, P.J. Alvarez, Effect of natural organic matter on toxicity and reactivity of nanoscale zero-valent iron, Water Res. 45 (2011) 1995–2001.

[17] J.N. Israelachvili, Intermolecular and Surface Forces, Academic Press, Waltham, MA, 2010.

[18] R.J. Hunter, L.R. White, Foundations of Colloid Science, Clarendon Press, Oxford, 1987.

[19] W.B. Russel, D.A. Saville, W.R. Schowalter, Colloidal Dispersions, Cambridge University Press, Cambridge, 1992.

[20] J. Gregory, Interaction of unequal double layers at constant charge, J. Colloid Interface Sci. 51 (1975) 44–51.

[21] D.B. Wagoner, R.F. Christman, G. Cauchon, R. Paulson, Molar mass and size of Suwannee River natural organic matter using multi-angle laser light scattering, Environ. Sci. Technol. 31 (1997) 937–941.

[22] D.J. Shaw, B. Costello, Introduction to Colloid and Surface Chemistry, Butterworth-Heinemann, Oxford, 1991.

[23] D.M. McKnight, E.W. Boyer, P.K. Westerhoff, P.T. Doran, T. Kulbe, D.T. Andersen, Spectrofluorometric characterization of dissolved organic matter for indication of precursor organic material and aromaticity, Limnol. Oceanogr. 46 (2001) 38–48.

[24] M. Grandbois, D.E. Latch, K. McNeill, Microheterogeneous concentrations of singlet oxygen in natural organic matter isolate solutions, Environ. Sci. Technol. 42 (2008) 9184–9190.

[25] V. Nicolosi, D. Vrbanic, A. Mrzel, J. McCauley, S. O'Flaherty, C. McGuinness, G. Compagnini, D. Mihailovic, W.J. Blau, J.N. Coleman, Solubility of $Mo_6S_{4.5}I_{4.5}$ nanowires in common solvents: A sedimentation study, J. Phys. Chem. B 109 (2005) 7124–7133.

[26] E.L. Sharp, P. Jarvis, S.A. Parsons, B. Jefferson, The impact of zeta potential on the physical properties of ferric–NOM flocs, Environ. Sci. Technol. 40 (2006) 3934–3940.